

Residual Stress Distribution in Alpha and Beta Phases of Mechanically Surface Treated TIMETAL LCB Determined by Energy-Dispersive X-Ray Diffraction

E. Maawad¹, H.-G. Brokmeier^{1,2}, L. Wagner¹, Ch. Genzel³, M. Klaus³

1 Institute of Materials Science and Engineering, Clausthal University of Technology, Clausthal-Zellerfeld, Germany

2 Helmholtz-Zentrum Geesthacht Center for Materials and Coastal Research, Geesthacht, Germany

3 Helmholtz-Zentrum Berlin (BESSY-II), Berlin, Germany

Abstract

TIMETAL LCB is a high-strength low cost solute lean beta titanium alloy. Good fatigue performance, high specific strength, excellent corrosion resistance and reasonable cost make this alloy most suitable for spring applications in transport. To improve fatigue life and damage tolerance, mechanical surface treatments are used to induce severe plastic deformation and residual compressive stresses in near-surface regions. The main aim of this investigation was to study the presence of residual stresses in both hexagonal close packed (hcp) α -phase and body centered cubic (bcc) β -phase as induced by shot peening (SP) and ball-burnishing (BB). To achieve such aim, energy dispersive X-ray diffraction (EDXRD) was used. The evaluation of complete diffraction spectra by EDXRD allows analyzing of α - and β -phases independently. Results clearly indicate significant differences in the amount of cold work and compressive residual stress states between α - and β -phases.

Keywords TIMETAL LCB, shot peening, ball-burnishing, residual stress, synchrotron radiation, neutron diffraction.

Introduction

TIMETAL LCB was introduced more than 10 years ago targeting automotive suspension spring applications. The nominal chemical composition of this alloy is Ti-1.5Al-6.8Mo-4.5Fe (wt. %). The formulation cost of this alloy is lowered by adding Mo and Fe in form of a ferro-molybdenum master alloy [1]. The high strength, low density, low Young's modulus and excellent corrosion resistance compared to steel make TIMETAL LCB an excellent choice for suspension springs in automotive. The first application dates back to the year 2000 when the rear axle of the Volkswagen Lupo FSI was equipped with LCB springs (Figure 1) [2].

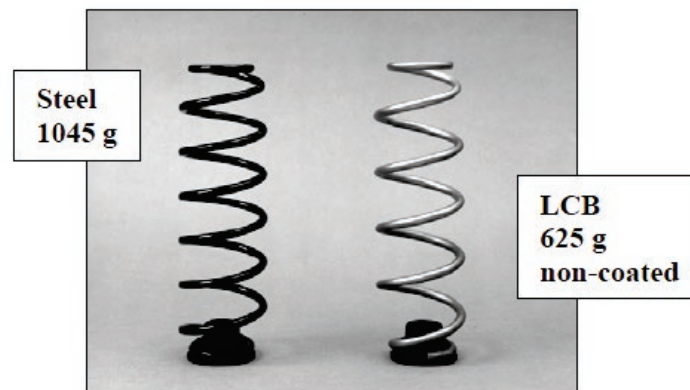


Figure1. TIMETAL LCB suspension spring vs. steel spring

To improve fatigue life and damage tolerance, mechanical surface treatments are used to induce severe plastic deformation and residual compressive stresses in near-surface regions. The influence of thermo-mechanical, thermal treatments and mechanical surface treatments on the fatigue behavior of TIMETAL LCB was already studied in detail [3, 4]. However, in previous work, the different responses of α - and β -phases to the SP- and BB-induced severe plastic surface deformations were not taken into account. Different residual stress states between α - and β -phases might give an explanation for the observation that the high-cycle fatigue (HCF) performance after SP and BB deteriorates relative to an electrolytically polished (EP) baseline. While residual stress measurements in TIMETAL LCB by the incremental hole drilling methods yielded only integral values of the various phases being present, residual stresses in individual phases can only be determined by diffraction methods such as X-ray diffraction (XRD) [5-7]. Laboratory XRD (Lab-XRD) in residual stress measurements usually takes into account only one reflection and therefore, is applicable for a material with high volume fractions of that particular phase being analyzed. In addition, relatively long counting times as well as good statistics are needed. Figure 2 shows an example of integrated residual stress depth-profile in TIMETAL LCB determined by incremental hole drilling (solid line) or Lab-XRD (dashed line) [6].

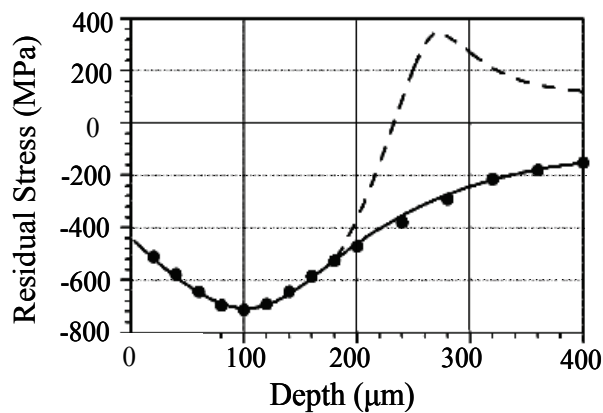


Figure 2. Residual stress depth-profile of the aged TIMETAL-LCB after SP [8]

This study was undertaken to determine in both α and β phases the full width at half maximum (FWHM) as a measure of the total induced dislocation density or work-hardening state and the residual stress depth-profiles as induced by SP and BB. To overcome the above described limitations in Lab-XRD, energy-dispersive X-ray diffraction (EDXRD) was applied.

Experimental Methods

TIMETAL LCB was received as swaged rod of 14.3 mm in diameter. The rod was unidirectionally rolled at 760°C to a thickness of 5 mm corresponding to a maximum deformation degree of about $\varphi = 1$. Blanks ($5 \times 20 \times 20 \text{ mm}^3$) were cut from the plate, recrystallization annealed at 760°C for 1 hour followed by water quenching. The blanks were final heat treated at 540°C for 8 hours followed by air cooling. Tensile tests were conducted on flat specimens having gauge length of 30 mm, width of 8 mm and thickness of 3 mm. Tests were done at ambient temperature with an initial strain rate of 10^{-3} s^{-1} . Specimens for EDXRD measurements were mechanically surface treated on both sides by applying SP or BB. SP was performed using cast steel (S330) having an average shot diameter of 0.80 mm and a hardness of 460 HV. Peening was performed to full coverage using an Almen intensity of 0.20 mmA. BB was performed by means of a conventional lathe using a hydrostatically driven tool (HG6) from Ecoroll Company. During BB, a hard metal ball ($\varnothing 6 \text{ mm}$) was pressed onto the surface applying a pressure of 300 bar. Residual stress measurements were performed by EDXRD at BESSY-II

in Berlin. The characteristic of the used beamline EDDI offers a white X-ray beam with energy range from 10 to 80 keV. The primary beam cross-section was defined as $0.5 \times 0.5 \text{ mm}^2$, the angular divergence in the diffracted beam was restricted by a double slit system with apertures of $0.03 \times 5 \text{ mm}^2$ to $\Delta\theta \leq 0.005^\circ$. The scattering angle was chosen to 8° considering the energy of the X-rays. EDXRD provides complete diffraction spectra for a fixed detector position. Any Bragg reflection could be obtained by a different X-ray energy (wavelength) which means the signal of any reflection belongs to a different depth in the sample as shown in Figure 3.

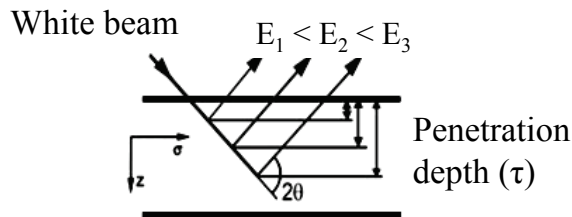


Figure 3. Relation between energy E and penetration depth τ (schematic)

Due to the limited usable energy range provided by the 7T multipole wiggler, the maximum information depth for titanium accessible in reflexion mode experiments is about $100 \mu\text{m}$. In order to measure stresses in deeper regions, two additional samples were prepared. Several layers of 100 to $150 \mu\text{m}$ were removed by EP to allow determining of the residual stress-depth distribution up to $600 \mu\text{m}$. Residual stresses were evaluated by means of the $\sin^2\psi$ method in steps of $\Delta\psi = 4^\circ$ up to 80° . The measured residual stress values were corrected using the equation which is described elsewhere [9]. A modified multi-wavelength approach [10] for any energy line $E_{(hkl)}$ gives an average penetration depth $\tau_{(hkl)}$ (Eq. 1).

$$\tau_{(hkl)} = (\tau_{(hkl) \min} + \tau_{(hkl) \max})/2 \quad (1)$$

where $\tau_{(hkl) \min}$ and $\tau_{(hkl) \max}$ are the minimum and the maximum penetration depths corresponding to the maximum and minimum tilting angles, respectively.

The diffraction elastic constants were calculated by the Kroener-Model [11].

Experimental Results and Discussion

The optical microstructure of the tested TIMETAL LCB is illustrated in Figure 4.

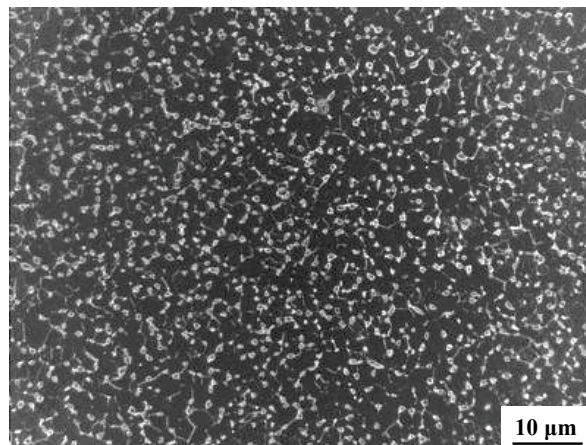


Figure 4. Microstructure of the aged TIMETAL LCB

The thermo-mechanical treatment resulted in equiaxed primary α -phase located at the grain boundary triple points of the β -grains. The size of the primary α -grains and their volume fraction were about 2 μm and 20%, respectively. During final heat treatment, fine secondary α -particles were precipitated out from the β -matrix leading to marked age-hardening [1]. Because of their small sizes, these secondary α -particles can only be seen by transmission electron microscopy (TEM). However, their presence changes the reaction of the β -phase to metallographic etching leading in optical microscopy (Fig. 3), to a dark appearance of the β - phase with embedded light primary α -grains.

The tensile properties of the tested material condition are listed in Table 1.

Table 1. Tensile properties of aged TIMETAL LCB

E (GPa)	YS (MPa)	UTS (MPa)	EI (%)	RA (%)
117	1260	1345	14.7	24.5

E = Young's modulus, YS = yield stress, UTS = tensile strength, EI = tensile elongation, RA = reduction of area

While the fine secondary α -particles cause the high values of YS and UTS, the tensile elongation is still quite high due to the fine β -phase dimensions (Fig. 4).

The applied severe plastic deformation during SP and BB leads to depth dependent gradients in the near-surface dislocation densities and resulting amount of cold work as seen by the full width at half maximum (FWHM) depth-profiles (Fig. 5).

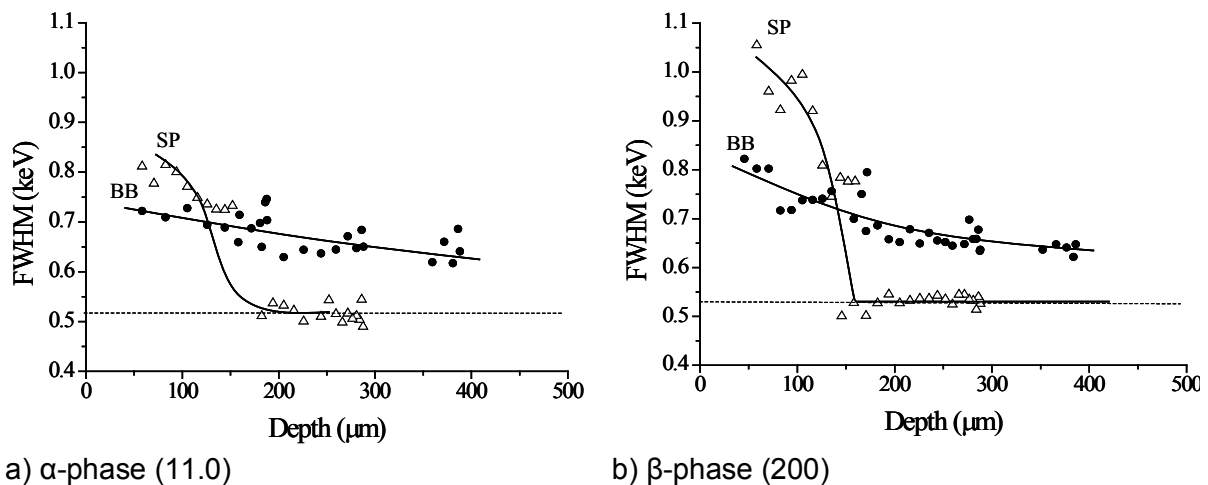


Figure 5. FWHM-depth profiles in TIMETAL LCB after SP and BB

As observed in both α - and β -phases, SP results in near-surface FWHM-values being greater than those after BB. Presumably, this is caused by the difference in ball size (0.8mm in SP vs. 6mm in BB). On the other hand, the penetration depth of elevated FWHM values in BB is much higher than in SP, this being also observed in micro-hardness depth profiles. Comparing the FWHM values between the α -phase (Fig. 5a) and β -phase (Fig. 5b), the greater amount of dislocation strengthening of the β -phase is quite evident.

Residual stresses as determined by EDXRD are illustrated in Fig. 6.

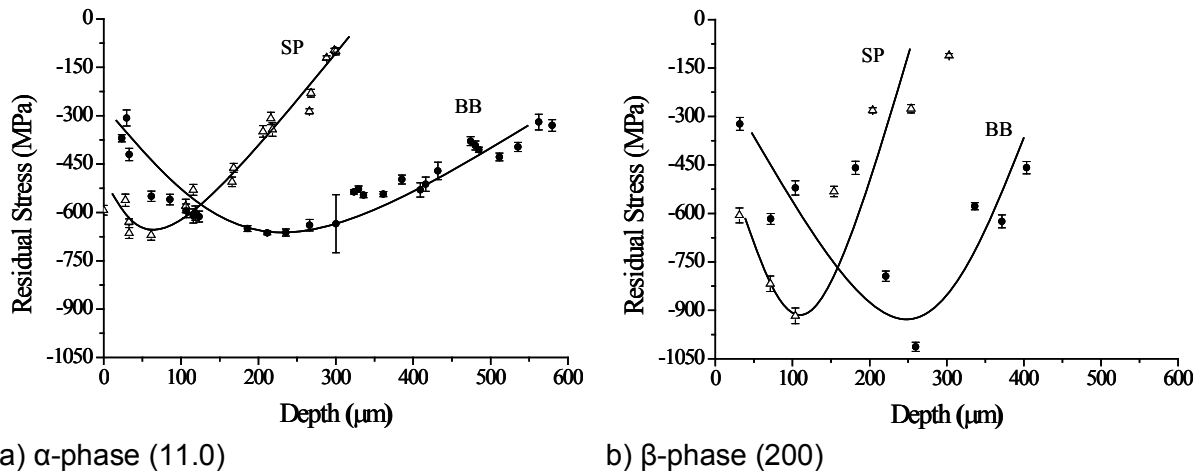


Figure 6. Residual stress-depth profiles in TIMETAL LCB after SP and BB

Generally, residual compressive stresses in near-surface regions in SP are higher than in BB (Fig. 5). This corresponds to the more pronounced severe plastic surface deformation of SP as shown in Figure 5. Accordingly, the penetration depth of residual compressive stresses in BB is much higher than in SP (Fig. 5). On average, residual compressive stresses in the β -phase are markedly higher than in the α -phase (compare Fig. 6b with Fig. 6a) this result being explained by the more marked work-hardening capability of the β -phase.

Discussion and Conclusions

The observed peak broadening after SP and BB being much more pronounced in the β -phase than in the α -phase can be explained by the presence of fine secondary α -particles in the β -matrix which are precipitated out during the final aging treatment. These hcp precipitates being incoherent to the bcc β -matrix not only lead to a homogenization of the slip distribution during plastic deformation but also stabilize the work-hardening states of the β -microstructure. In contrast, the correspondingly low strength of the primary α -phase is not affected by the final heat treatment. Very similar to the strength differential after severe plastic deformation between α -phase and β -phase, the residual compressive stresses after SP and BB in the age-hardened β -phase are also much higher than in the α -phase.

Work on unaged TIMETAL LCB regarding FWHM- and residual stress measurements after SP and BB is underway to clarify the effect of aging on the β -phase properties

Acknowledgements

The authors are indebted to the German Research Foundation (DFG) for financial support through BR961/5-2 and WA 692/32-2. This work was additionally supported by the European Community - Research Infrastructure Action under the FP6 "Structuring the European Research Area" Programme (through the Integrated Infrastructure Initiative "Integrating Activity on Synchrotron and Free Electron Laser Science - Contract R II 3-CT2004-506008").

References

- [1] Y. Kosaka, S. P. Fox, K. Faller and S. H. Reichman, *Properties and Processing of TIMETAL LCB*, Journal of Materials Engineering and Performance, Vol. 14 (6) (2005), pp 792.
- [2] O. Schauerte, *Titanium in Automotive Production*, Journal of Advanced Engineering Materials, Vol. 5 (6) (2003), pp 411.
- [3] J. Kiese, W. Walz and B. Skrotzki, *Shot Peening to Enhance Fatigue Strength of TIMETAL LCB for Application as Suspension Springs*, in: Proc. of the 10th Int. Conference on Titanium (G. Lütjering and J. Albrecht, eds.), Hamburg, Germany, 2003, pp. 3043.
- [4] T. Ludian, M. Kocan, H. J. Rack and L. Wagner, *Residual Stress-Induced Subsurface Crack Nucleation in Titanium Alloys*, Journal of Materials Research, Vol. 97 (2006) 10, pp 1425.
- [5] I. Altenberger, Y. Sano, M. Cherif, I. Nikitin and B. Scholtes, *Residual Stress State and Fatigue Behaviour of Laser Shock Peened Titanium Alloys*, Materials Science Forum Vols. 524-525 (2006), pp 129.
- [6] M. Kocan, H.J. Rack and L. Wagner, *Fatigue Performance of Metastable Beta Titanium Alloys: Effects of Microstructure and Surface Finish*, Journal of Materials Engineering and Performance, Vol.14 (6) (2005), pp 765.
- [7] M. Kocan, H.J. Rack and L. Wagner, *Effect of Age-Hardening and Mechanical Surface Treatments on HCF Performance of TIMETAL LCB for Application as Suspension Springs*, Shot Peening and Other Mechanical Surface Treatments, Procs. ICSP9, V. Schulze (ed.), (2005) pp 320.
- [8] P. Withers and H. D. Bahadreshia, *Residual stress, Part 1 – Measurement techniques*, Materials Science and Technology, Vol. 17 (2001), pp 355.
- [9] M.G. Moore and W.P. Evans, *Mathematical Correction for Stress in Removed Layers in X-Ray Diffraction*, Residual Stress Analysis, SAE Transaction, Vol. 66 (1958), pp 340.
- [10] Ch. Genzel, C. Stock and W. Reimers, *Application of energy-dispersive diffraction to the analysis of multiaxial residual stress fields in the intermediate zone between surface and volume*, Journal of Materials Science and Engineering A, Vol. 372 (2004), pp 28.
- [11] E. Kroener, *Berechnung der elastischen Konstanten des Vielkristalls aus den Konstanten des Einkristalls*, Z. Physik, Vol. 151 (1958), pp 504.